Journal of Contaminant Hydrology 241 (2021) 103797

Contents lists available at ScienceDirect

Journal of Contaminant Hydrology

journal homepage: www.elsevier.com/locate/jconhyd

Dynamics of nitrous oxide with depth in groundwater: Insights from ambient groundwater and laboratory incubation experiments (Hesbaye chalk aquifer, Belgium)

Olha Nikolenko [a,*], Serge Brouyère [a,*], Pascal Goderniaux [b], Tanguy Robert [a,c,d], Philippe Orban [a], Alberto V. Borges [e], Anna Jurado [f], Maxime Duvivier [a], Cedric Morana [e]

[a] University of Liège, Urban and Environmental Engineering Department, Hydrogeology and Environmental Geology, Aquapôle, 4000 Liège, Belgium
[b] Geology and Applied Geology, Polytech Mons, University of Mons, Mons, Belgium
[c] F.R.S.-FNRS (Fonds de la Recherche Scientifique), 1000 Brussels, Belgium
[d] VIVAQUA, Direction de la Production, Hydrogéologie, 1000 Brussels, Belgium
[e] Chemical Oceanography Unit, University of Liège, Liège, Belgium
[f] GHS, Institute of Environmental Assessment and Water Research (IDAEA), Severo Ochoa Excellence Center of the Spanish Council for Scientific Research (CSIC), Barcelona, Spain

ARTICLE INFO

Keywords:
Greenhouse gases
Groundwater
N stable isotope analysis
Low-flow sampling
Nitrification
Denitrification

ABSTRACT

Aquifers under agricultural areas are considered to be an indirect source of nitrous oxide emission (N_2O) to the atmosphere, which is the greenhouse gas (GHGs) characterized with the highest global warning potential and acts as a stratospheric ozone depletion agent. Previous investigations performed in the Cretaceous Hesbaye chalk aquifer in Eastern Belgium suggested that the dynamics of N_2O in the aquifer is controlled by overlapping biochemical processes such as nitrification and denitrification. The current study aims to obtain better insight concerning the factors controlling the distribution of N_2O concentration along a vertical dimension in the aquifer, and to capture and quantify the occurrence of nitrification and denitrification processes in the groundwater system. Low-flow groundwater sampling technique was undertaken at different depths in the aquifer to collect groundwater samples aiming at obtaining information about ambient aquifer hydrogeochemical conditions and their effect on the accumulation of GHGs. Afterwards, laboratory stable isotope experiments, using NO_3^- and NH_4^+ compounds labeled with heavy ^{15}N isotope, were applied to quantify the rates of nitrification and denitrification processes. Ambient studies suggest that the occurrence of N transformation was related to denitrification while laboratory incubation experiments did not detect it. Such controversial results might be explained by the discrepancy between real aquifer conditions and lab design studies. Thus, additional *in situ* tracer experiments should be carried out in areas where natural groundwater fluxes do not flush the injected tracer too rapidly. In addition, it would be useful to conduct microbiological studies to obtain better insight into the nature of subsurface biofilm biotope.

1. Introduction

One of the major challenges of this century is to find the balance between intensive agricultural production and related environmental damages such as the contribution to anthropogenic GHGs emissions and climate change, or the deterioration of water resources and soil (Fisher et al., 2018). Inorganic and organic N fertilizers, intensively used for decades to increase annual harvest, have contributed to changes in the N biogeochemical cycle (Davidson, 2009). In particular, this change has led to increased atmospheric concentrations of nitrous oxide (N_2O) by ~122% in comparison to the preindustrial period with a continuous annual raise by 0.2–0.3% (Anderson et al., 2010; World Meteorological Organization, 2018). N_2O is a greenhouse gas (GHGs) which is characterized by a warming potential 298 times higher than carbon dioxide (CO_2) and an average atmospheric longevity of 114 years (IPCC, 2016).

Pollution of groundwater under agricultural landscapes with N species makes aquifers a potential source of N_2O emission to the atmosphere in areas of groundwater discharge or through pumping activities

* Corresponding authors.
E-mail address: nikolenko_olha@ukr.net (O. Nikolenko).

https://doi.org/10.1016/j.jconhyd.2021.103797
Received 15 September 2020; Received in revised form 27 February 2021; Accepted 12 March 2021
Available online 15 March 2021

(Fox et al., 2014; Gardner et al., 2016; Jurado et al., 2018). There is still large uncertainty regarding the quantification of N_2O emission from aquifer systems since most approaches, used for the calculation the emission factor from groundwater, assume that they act only as a transport media without any internal N transformation processes (Zhou et al., 2019). That is why it is important to improve our understanding of the dynamics of N in groundwater, which is highly variable in space and time and might lead to the accumulation of N_2O in the subsurface (Hinkle and Tesoriero, 2014) and indirectly in the atmosphere. Differentiating the specific contribution of different biogeochemical pathways to N_2O production at local to regional scales can help to introduce process-oriented mitigation measures that will contribute to decrease global N_2O emission (Guo et al., 2018).

This study attempts to characterize the dynamics of N_2O in one of the largest chalk aquifer located under agricultural areas in the Walloon Region (Belgium). Based on regional investigations in this groundwater body, it was assumed that the availability of N_2O in the chalk aquifer was governed by both nitrification and denitrification processes (Nikolenko et al., 2019). In order to test this hypothesis, further explorations here focus on upper and lower parts of the aquifer assuming that they were presumably different in terms of physical-chemical and/or biochemical conditions. Those differences may actually explain the mixed origin of N_2O. Therefore, the objectives of this study are: 1) to obtain better insight related to the distribution of N compounds and their isotopes with depth in the chalk aquifer; 2) to characterize in details the effect of changing hydrogeochemical conditions on N_2O production/consumption processes and 3) to estimate of the rates of nitrification and denitrification processes in the aquifer.

2. Materials and methods

2.1. Study site

The studied aquifer is located in Cretaceous chalky geological formations in the Eastern Belgium (Brouyère et al., 2004; Orban et al., 2010; Goderniaux et al., 2015). Two sites (Bovenistier and SGB), allowing access to different aquifer depths, were selected for the studies. Both are equipped with multilevel piezometers, which characteristics and investigated depth intervals are shown in Fig. 1. During the investigations, upper and lower groundwater layers were examined in each piezometer. For the sake of convenience in further discussion, all of the sampling points (*i.e.*, depth intervals which were sampled) are numbered from 1 to 10, as indicated in Fig. 1 along the left side of each piezometer.

2.2. Sampling procedure

Information regarding the hydrochemical conditions, concentrations of N compounds and their isotopic and isotopomer signals, used to describe the nature of N_2O dynamics, was obtained by chemical and isotope analyses of groundwater samples. Those were collected using a low-flow sampling technique during the summer (June 2019) and winter (November 2019) campaigns. Samples were collected at the end of a low flow pumping (240 mL/min) stage performed at each location until the stabilization of electrical conductivity (EC) and pH, using a Solinst bladder pump model 407 SS 1.66`` Dia. It was assumed that stabilization occurred when five consecutive measurements for EC and pH did not differ by ±2% and ± 0.1 units, respectively.

2.3. Exploration of the variability of N compounds and their isotopes with depth

The results of isotopic and chemical analyses of groundwater samples consist of:

1) total nitrate (NO_3^-) and boron (B) dual isotope plots for both SGB and Bovenistier sites;
2) comparative vertical distribution profiles of NO_3^-, N_2O and N isotopes, for the summer and winter campaigns and for each of the studied sites individually.

Dual isotope plots help to address the question whether changes in N isotope and isotopomer values along the profiles are related to the ongoing N_2O production/consumption processes or are due to differences in the isotopic signatures of the initial substrate sources. The analysis of ^{11}B was performed only for groundwater samples collected in summer. Consequently, the conclusions regarding the origin of N in winter samples will be made both by examining NO_3^- dual isotope plots and considering the corresponding results of $\delta^{11}B$ analyses from summer samples. Comparative vertical distribution profiles are used to examine covariations between N compounds and their isotopes with depth which helps to understand N_2O dynamics in the aquifer.

2.4. Estimation of the rates of nitrification and denitrification processes

Two N stable isotope labeled experiments were conducted in order to

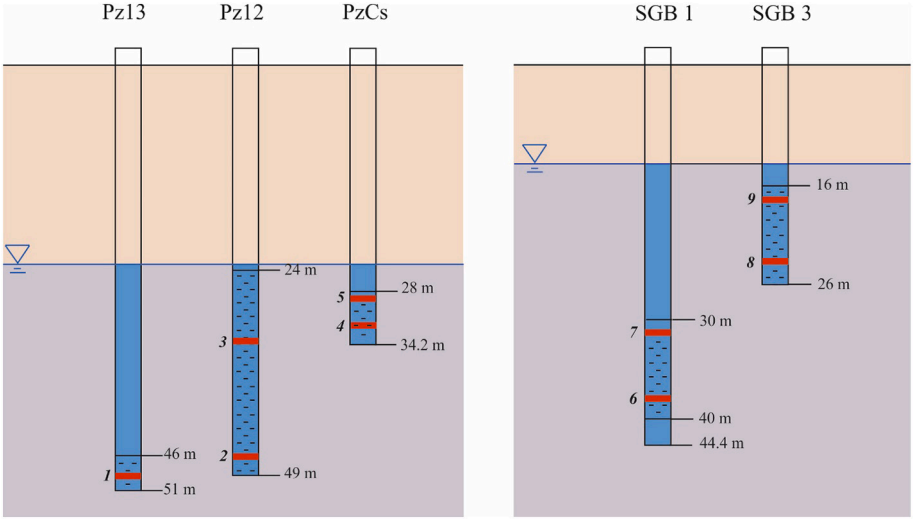

Fig. 1. Piezometers and sampling depths at the Bovenistier (left) and SGB (right) sites. Sampling points are numbered from 1 to 10, as indicated in bold and italics on the left side of each piezometer. The groundwater level value is not indicated, since it was not stable between summer and winter campaigns.

estimate the rates of nitrification and denitrification processes in groundwater. For this purpose, groundwater was collected at different depths of the aquifer at Bovenistier and SGB sites (see sampling points on Fig. 1 section 2.1.) during the winter campaign. From each sampling point, 4 water samples of 50 mL each were collected and stored in borosilicate serum vials sealed without headspace using a butyl rubber stopper and an aluminum seal. Half of them were used for nitrification incubation experiment and another half for denitrification incubation experiment by addition of ^{15}N labeled compounds. It should be emphasized that this experiment provides the information about the potential rates of nitrification and denitrification because the addition of the ^{15}N labeled compounds (substrates for denitrification and nitrification processes) increases their concentrations relative to its *in situ* values.

Nitrification rates were determined in headspace-free serum vials spiked with ^{15}N-labeled NH_4Cl (99 atom% ^{15}N) by measuring the changes in $\delta^{15}N\text{-}NO_3^-$ values resulting from the oxidation of the $^{15}NH_4^+$ which is a substrate for nitrification. Since the results of chemical analysis showed the ambient concentration of NH_4^+ in groundwater was below the detection limit, it was decided to amend water samples with an excess of $^{15}N\text{-}NH_4^+$ in order to reach the final concentration of ~2 mg/L of NH_4^+. Similarly, denitrification rates were determined in headspace-free serum vials amended with ^{15}N-labeled KNO_3 (25 atom% ^{15}N) by observing the changes in $^{15}N\text{-}N_2O$ and $^{15}N\text{-}N_2$ isotopic signatures expecting the consumption of added isotopically enriched $^{15}N\text{-}NO_3^-$ (25 atom% ^{15}N) which is a substrate for denitrification. Considering that the background concentration of NO_3^- in groundwater vary from 0 to 52.5 mg/L (based on the results obtained from summer campaign), the amount of injected $^{15}N\text{-}NO_3^-$ was defined aiming to double the concentration of NO_3^- at each location. Amendments were made by injecting the tracer solutions through the septa of borosilicate glass vials.

The magnitudes of nitrification and denitrification processes were measured during 24 h and 48 h long experiments, respectively, each of which consisted of four time spans with 2 vials used for each time span (duplicates). The vials were incubated in the dark under 10 °C which corresponds to the mean *in situ* temperature of groundwater at the time of sampling. Both incubations started just after tracer injections. At the beginning of the incubation experiments, an addition of 200 μL of a saturated solution of $HgCl_2$ in two vials was performed to inhibit microbiological activity in order to have reference values of initial T_0 $^{15}N\text{-}NO_3^-$, $^{15}N\text{-}N_2O$ and $^{15}N\text{-}N_2$ isotopic values. For nitrification, further inhibitions of microbiological activity took place in 2 subsequent vials in the time course after 6 h, 12 h, 18 h and 24 h intervals. For denitrification, the intervals after which inhibition was performed in the respective vials were established at 6 h, 12 h, 24 h and 48 h.

The magnitude of nitrification and denitrification were estimated based on the formula provided by Hama et al. (1983) and adapted for the quantification of NO_3^- or N_2O and N_2 production rates:

$$P = \frac{C \times (a_{is} - a_0)}{(t \times (a_s - a_0))} \quad (3)$$

where P is the production rate of a particular compound (*nmol/L/h*), C is the initial (background) concentration of this compound (*nmol*), a_{is} is the atom% of ^{15}N in this compound in incubated samples at the end of each incubation interval, a_0 is the atom% of ^{15}N in the studied compound at the beginning of incubation experiment (T_0) just after the addition of a tracer, a_s is the atom% of ^{15}N in a substrate for nitrification ($^{15}NH_4^+$) or denitrification ($^{15}NO_3^-$) after the addition of a tracer at the beginning of incubation and t is incubation time (*h*).

2.5. Analytical methods

The analyses of groundwater samples for NO_3^-, NO_2^- and NH_4^+ was performed at the Hydrogeology Laboratory of the University of Liège (Belgium) by means of aqueous phase ion chromatography *via* specific ion exchange resin and a conductivity detector.

The concentrations of dissolved N_2O was measured at the Chemical Oceanography Unit of the University of Liège (Belgium) with the headspace equilibration technique (20 ml of N_2 headspace in 50 ml serum bottles) and a gas chromatograph equipped with electron capture and flame ionization detectors (SRI 8610 GC-ECD-FID), as described in detail by Borges et al. (2015). The SRI 8610 GC-ECD-FID was calibrated with CH_4:CO_2:N_2O:N_2 mixtures (Air Liquide Belgium) of 0.2, 2.0 and 6.0 ppm N_2O and of 1, 10 and 30 ppm CH_4. The reproducibility of measurements was ±3.2% for N_2O concentration analysis.

The stable isotope analyses of N_2O present in ambient groundwater samples were conducted using an off-axis cavity ringdown spectroscopy (OA-ICOS) (Los Gatos Research) instrument for the measurements of $\delta^{15}N^{\alpha}$, $\delta^{15}N^{\beta}$, $\delta^{18}O$ of N_2O at the Chemical Oceanography Unit of the University of Liège (Belgium), and the ^{15}N-site preference (SP, in ‰) was calculated as the difference between central ($\delta^{15}N^{\alpha}$) and peripheral ($\delta^{15}N^{\beta}$) ^{15}N enrichment of the linear N_2O molecule ($\delta^{15}N^{\alpha} - \delta^{15}N^{\beta}$). A 20 ml helium (He) headspace was created in the 250 ml bottles ~24 h before the analysis in order to assure equilibration between gas and dissolved N_2O. Headspace samples were injected into a custom-built purge and trap device (He flow: 120 ml min-1) consisting of a CO_2 trap (soda lime), a water trap (magnesium perchlorate) and a stainless steel loop immersed in liquid nitrogen to trap N_2O. Volume of headspace injection was adapted as function of the N_2O concentration in every sample in order to minimize concentration-dependent effect as much as possible (Wassenaar et al., 2018). Data was calibrated against calibration curves obtained with several injection at increasing concentration (typically 8) of an international reference material (USGS52, $\delta^{15}N^{\alpha}_{air} = 13.52‰$, $\delta^{15}N^{\beta}_{air} = -12.64‰$, $\delta^{18}O_{smow} = 40.14‰$) and an in-house N_2O standard provided by Air Liquide Belgium ($\delta^{15}N^{\alpha}_{air} = 0.47‰$, $\delta^{15}N^{\beta}_{air} = 1.41‰$, $\delta^{18}O_{smow} = 37.63‰$) and previously calibrated by the Tokyo Institute of Technology. Data calibration was performed as described in Wassenaar et al. (2018). Analytical precision was 0.5‰, 1.2‰ and 1.2‰ for $\delta^{15}N^{\alpha}_{air}$, $\delta^{15}N^{\beta}_{air}$, and $\delta^{18}O_{smow}$, respectively.

The $\delta^{15}N\text{-}NO_3^-$ and $\delta^{18}O\text{-}NO_3^-$ isotopes analyses were conducted using an off-axis cavity ringdown spectroscopy (OA-ICOS) (Los Gatos Research) instrument (University of Liège, Belgium) applying Cd-Azide reduction method to quantitatively converts NO_3^- to N_2O (McIlvin and Altabet, 2005; Ryabenko et al., 2009; Wassenaar et al., 2018). After chemical conversion of NO_3^- to N_2O, the resulting gas was analyzed with the above mentioned laser isotope analyzer using the same analytical setup as for N_2O isotopes analysis. Samples and standards (IAEA-NO3, $\delta^{15}N\text{-}NO_3^- = 4.7‰$, $\delta^{18}O\text{-}NO_3^- = 25.6‰$) were normalized to the same concentration (20 μmol L-1) before the initiation of the Cd-azide reduction protocol following the recommendation of Wassenaar et al., 2018. Typical precision for $\delta^{15}N\text{-}NO_3^-$ was better than 0.6‰ and for $\delta^{18}O\text{-}NO_3^-$ was better than 1.8‰. The $\delta^{11}B$ measurements in groundwater samples was performed using sector field-inductively coupled plasma-mass spectrometry (SF-ICP-MS) according to the procedure described by Tirez et al., 2010. The precision on the quality control sample (NBS 951) that was measured along in this run amounts ±2.6‰.

Groundwater dissolved gases (N_2O and N_2) from incubation samples were extracted using the headspace equilibration technique with helium (He) filling the headspace (20 ml of He headspace in 50 ml serum bottles). The $\delta^{15}N\text{-}N_2O$ values were determined on a dual-inlet isotope ratio mass spectrometer (Stable Isotope Facility, UC Davis, Davis, CA) as described by Mosier and Schimel (1993). Note that only the samples from 5 locations out of 9 (Pz 13 (*1*), Pz12 (*3* and *5*) and SGB (*4* and *6*)) were sent for the $^{15}N\text{-}N_2O$ isotope analyses. The $\delta^{15}N\text{-}N_2$ was estimated by isotope ratio mass spectrometer (delta V plus, ThermoScientific) (volume injected in the mass spectrometer: 50 μL). Typical precision for $\delta^{15}N\text{-}N_2$ analysis with the IRMS was better than 0.2‰.

3. Results

3.1. Sources of N compounds in groundwater

According to the obtained results, the origin of N in groundwater samples at the Bovenistier site during the summer period (Fig. 2) was attributed to 2 major sources: manure, the isotope signal of which was dominant at the shallowest sampling point *5* (PzCs), and NH_4^+ fertilizers identified at the deeper studied points *4* (PzCs), *3* and *2* (both in Pz12) (Fig. 2).

In the absence of $\delta^{11}B$ samples for the winter campaign, it was more difficult to distinguish the N sources in this dataset. For example, the sample *5w* indicates NO_3^- isotopic values typical for both fertilizers and sewage. The sample *4w* exhibits NO_3^- isotopic signals typical for denitrification process as *4* and *4w* are located along the denitrifying line with a slope 1:1. Though the small enrichment factor (2.15‰), which is not typical for denitrification under natural conditions, is observed here, the denitrification cannot be excluded in case the studied system is substrate limited and high microbiological activity is present (Clark, 2015). The presence of the first condition can be supported by the two fold decrease in the concentration of NO_3^- between *4* and *4w*. As for the second one, additional microbiological studies are required in order to detect the activity of denitrifiers. Nevertheless, according to Jahangir et al. (2013) denitrifier functional genes are ubiquitous in groundwater systems. Despite the fact that *3* and *3w* are located along the denitrifying line with a slope 2:1, denitrification cannot be claimed in this case. It is related to the fact that two points are located too far away from each other which gives extremely high enrichment factor taking into account the absolute absence of change in the concentration of NO_3^- (Fig. 2). At point *1* (Pz13) NO_3^- is detected only in the winter, and its isotope signature fall out of the ranges typically attributed to the considered N sources.

At the SGB site (Fig. 3) samples *8* and *9* (SGB3) that belong to the shallower part of the aquifer show isotopic values that can be attributed to different N sources, while the samples *6* and *7* (SGB1) that belong to the deeper part of the aquifer fall in the sewage interval. During the summer campaign, samples *8* and *9* can be associated with household sewage and manure, respectively. In winter, the same samples fall into the ranges typical for household sewage and NH_4^+ fertilizers. Samples *7* show NO_3^- and B isotope values typical for both NH_4^+ fertilizers and household sewage during summer and winter periods. Sample *6w* demonstrates N isotopic signatures which might be associated with denitrification processes as *6* and *6w* fall along the denitrifying line with slope 2:1. The occurrence of denitrification is supported by the drastic decrease in the concentration of NO_3^- between *6* and *6w* (Fig. 3) and the reasons described in the above paragraph for points *4* and *4w*.

3.2. Depth specific distribution of N compounds and their isotopes

In this section changes in vertical variations of the concentrations of N compounds, N isotopic signatures and dissolved oxygen (DO) at the SGB and Bovenistier sites for the summer and winter periods are discussed.

Groundwater samples from the SGB site show concentrations of N-N_2O which exceed the equilibrium with the atmosphere concentration (0.3 μgN/L) (Hasegawa et al., 2000). In winter N_2O concentrations were higher (12.6 ± 2.9 μgN/L) in comparison to the summer (8.2 ± 1.5 μgN/L). The SGB1 piezometer showed that the concentration of N-N_2O was higher in the deepest part of the piezometer (point *6*–9.9 μgN/L and 14.5 μgN/L) than in its upper part (point *7*–6.4 μgN/L and 11.6 μgN/L) in the summer and winter campaigns, respectively. The *SGB3* piezometer did not indicate any significant difference in N-N_2O concentration with depth for the summer campaign. However, for the winter campaign the upper sampling location (sample *9)* showed a concentration almost

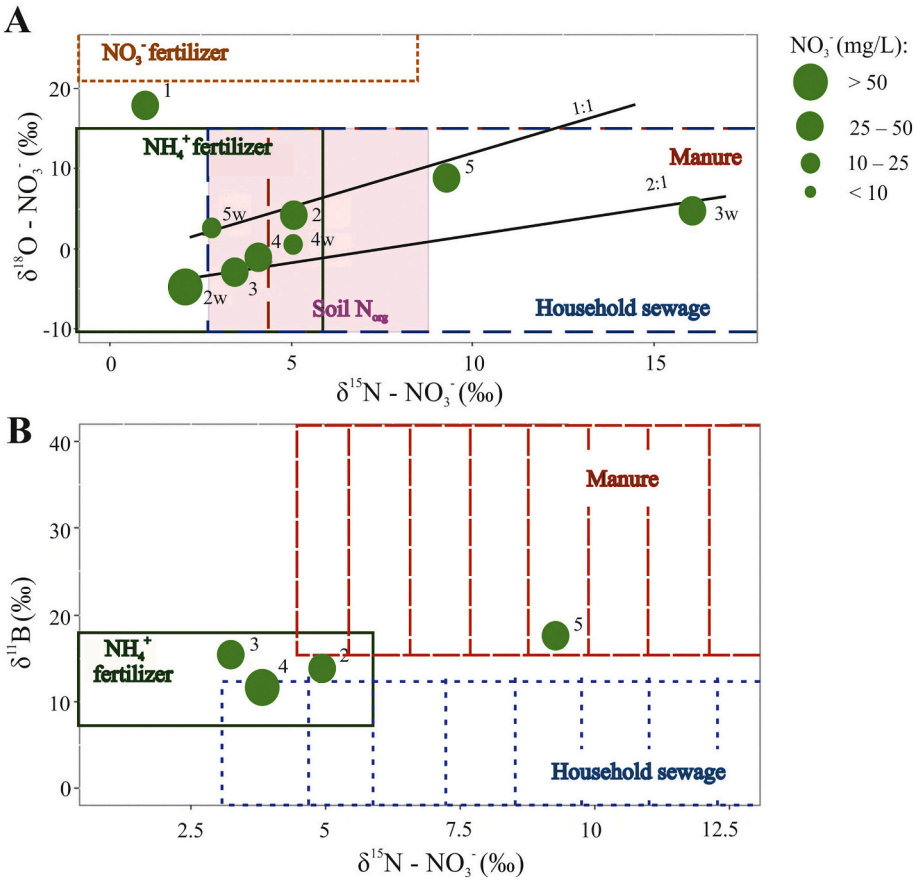

Fig. 2. NO_3^- and B dual isotope plots of groundwater samples collected at Bovenistier site. Graph A includes the data from summer and winter and graph B includes the data from summer only. The letter "w" next to the number of sampling location means that the sample was collected in the winter. Green circles of different size indicate different concentrations of NO_3^- in groundwater samples. The ranges of isotopic compositions for NO_3^- and B sources (boxes drawn in the graphs) are derived from Michener and Lajtha (2007), Xue et al. (2009) and Widory et al. (2004). Ratios of $\delta^{15}N$ and $\delta^{18}O$ of NO_3 used to draw denitrification lines are taken from Koba et al., 2009. (For interpretation of the references to colour in this figure legend, the reader is referred to the web version of this article.)

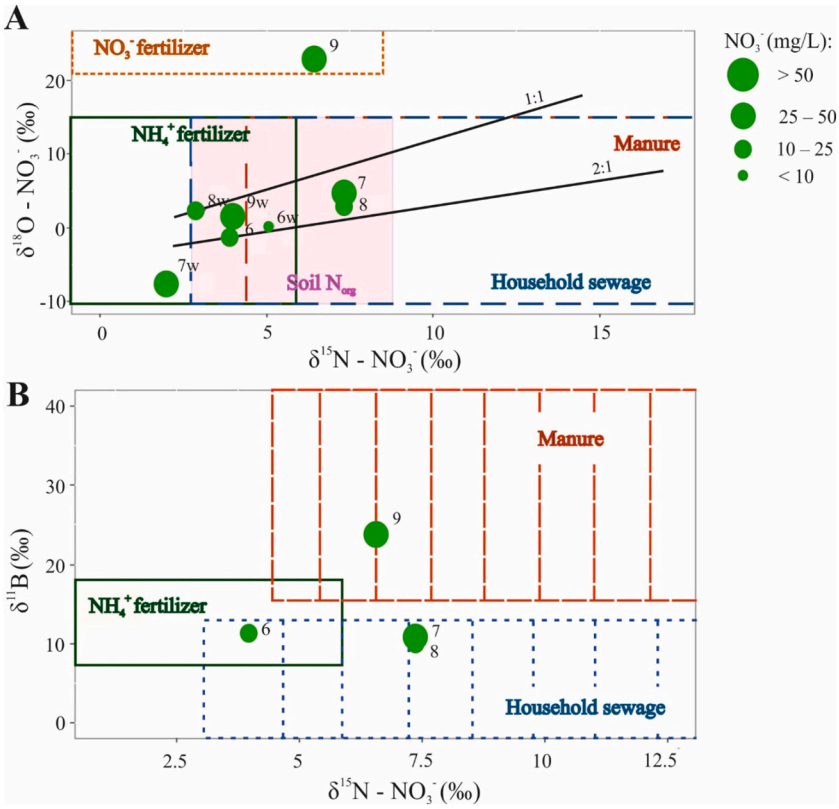

Fig. 3. NO_3^- and B dual isotope plots of groundwater samples collected at SGB site. Graph A includes the data from summer and winter and graph B includes the data from summer only. The letter "w" next to the number of sampling location means that the sample was collected in the winter. Green circles of different size indicate different concentrations of NO_3^- in groundwater samples. The ranges of isotopic compositions for NO_3^- and B sources (boxes drawn in the graphs) are derived from Michener and Lajtha (2007), Xue et al. (2009) and Widory et al. (2004). Ratios of $\delta^{15}N$ and $\delta^{18}O$ of NO_3 used to draw denitrification lines are taken from Koba et al., 2009. (For interpretation of the references to colour in this figure legend, the reader is referred to the web version of this article.)

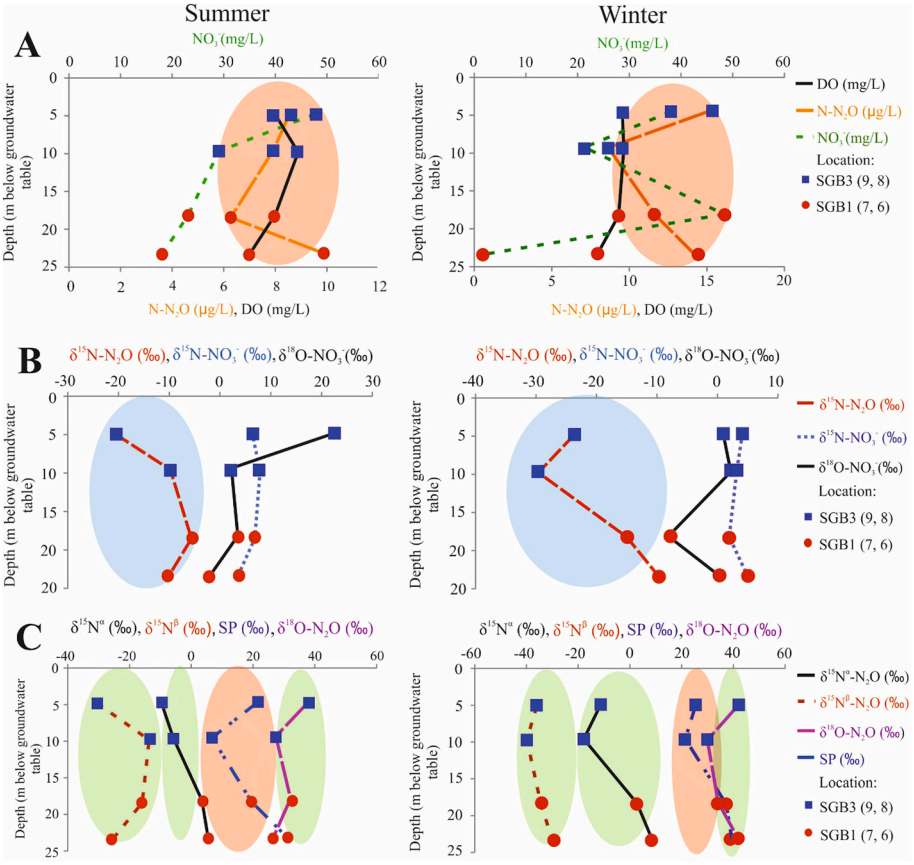

Fig. 4. Vertical distributions of N compounds, N isotopes and DO at the SGB site during summer and winter periods. Colorful circles highlight distributions of parameters compared in the section 3.2.

two times higher (15.5 μgN/L *versus* 8.6 μgN/L) compared to the deeper sampling location (sample *8*).

At the SGB site the concentrations of NO_3^- decreased with depth, but they showed significant variations between the summer and winter sampling campaigns. The shallower sampling points *8* and *9* showed concentrations of 28.7 mg/L and 47.9 mg/L mg/L in the summer and 21.5 mg/L and 38.3 mg/L, in the winter. The deeper samples *6* and *7* showed NO_3^-concentrations 23.5 mg/L and 18.3 mg/L in the summer, and of 48.7 mg/L and 1.56 mg/L in the winter. The concentrations of DO were in a range between 7.0 mg/L to 9.6 mg/L, decreasing with depth during both sampling periods.

The SP and N-N_2O results (red circles, Fig. 4 A and C) changed in the same direction along the depth profile both in the summer and winter campaigns, with the exception of location *7* for N-N_2O. This indicates the absence of N_2O reduction processes (Ostrom et al., 2007). The similarity between N-N_2O and δ^{15}N-N_2O evolutions (blue circle, Fig. 4 B) in the winter campaign also indicates that N_2O is not reduced. Such a similarity is not observed for the summer sampling campaign, which in this case might evidence N_2O reduction.

Moreover, data from the summer campaign show a strong covariation with depth between of δ^{15}N-N_2O and $\delta^{15}N^{\beta}$-N_2O (green circle, Fig. 4 C) which suggests close dependence between these two parameters. The $\delta^{15}N^{\alpha}$-N_2O enrichment increased with depth, while the δ^{18}O-N_2O (green circles, Fig. 4 C) decreased slightly.

The winter campaign data show that δ^{15}N-N_2O, $\delta^{15}N^{\alpha}$-N_2O, $\delta 15N^{\beta}$-N_2O and δ^{18}O-N_2O (green circles, Fig. 4 C) parameters exhibited similar vertical distribution patterns, along the vertical profile with more pronounced increase of $\delta^{15}N^{\alpha}$-N_2O with depth. This observation suggests that δ^{15}N-N_2O signature might be either influenced by production processes solely or influenced to the same extent with both N_2O production and reduction processes.

All samples collected at Bovenistier showed N-N_2O concentrations exceeding the equilibrium with the atmosphere. Similarly to the SGB site, the concentration of this gas was higher in the winter (10.5 μgN/L ± 1.7 μgN/L) than in the summer (8.6 μgN/L ± 1.3 μgN/L). For the summer campaign, samples *4* and *5* (PzCs) showed higher concentrations of N-N_2O 10.16 μgN/L and 9.26 μgN/L, respectively, in comparison to *3* and *2* (Pz12) where its concentrations were nearly the same (around 7 μgN/L). During the winter campaign, N-N_2O concentrations varied vary between 10.7 μg N/L and 12.4 μgN/L at all of the sampling points with higher concentrations observed at the bottom parts of piezometers – sampling points *4* and *2*. During the winter campaign N_2O was detected at a concentration of 7.7 μgN/L at the deepest sampling location *1* (Pz13) but in the summer campaign the concentration there was below the detection limit.

During the summer campaign, the concentration of NO_3^- did not change noticeably between point *4* and *5* (PzCs) (> 40 mg/L), but it varied between samples *3* and *5* (47.8 mg/L *vs* 37.0 mg/L) located respectively in the shallow and deep part of Pz12. During this period, NO_3^- was not detected in the sample collected at location *1* in Pz13. In the winter, the NO_3^- concentration was almost two times lower at location *5* (24.2 mg/L) than at location *4* (46.2 mg/L). At the same period, there was no significant difference in NO_3^- between locations *2* and *3* (> 40 mg/L) and the concentration of NO_3^- was 47.9 mg/L at point *1* in Pz13. The concentration of DO varied from 1.5 mg/L to 9.9 mg/L.

At Bovenistier, variations with depth of N-N_2O and SP (red circles, Fig. 5 A and C) were different for both winter and summer periods. However, these differences are not significant enough to conclude on the possible occurrence of N_2O reduction. At the same time, the similarity observed between N-N_2O and δ^{15}N-N_2O (blue circle, Fig. 5 B) profiles for winter (except for the deepest sampling point at Pz12 and Pz13) indicates the absence of N_2O reduction in the shallower part of the aquifer

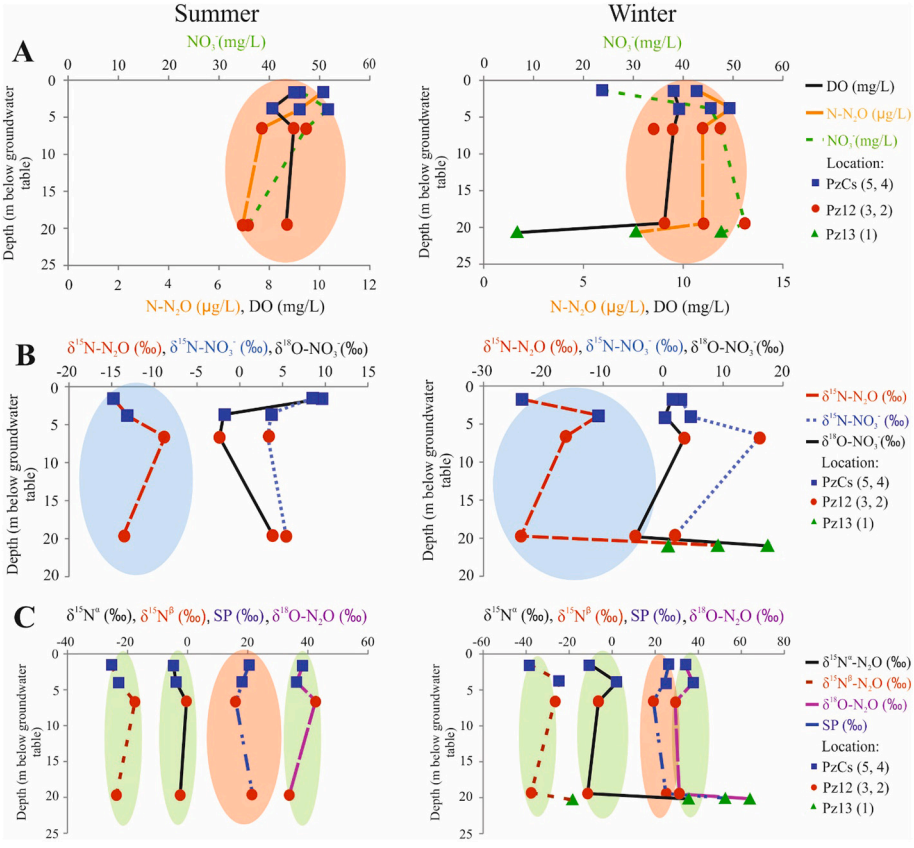

Fig. 5. Vertical distributions of N compounds, N isotopes and DO at the Bovenistier site during summer and winter periods. Colorful circles highlight distributions of parameters compared in the section 3.2.

and its occurrence in the deepest part. N_2O reduction processes at the bottom part of the aquifer are also supported by the positive value of $\delta^{15}N\text{-}N_2O$ (9.2‰) and the high $\delta^{18}O\text{-}N_2O$ value (66.0‰). During the summer campaign, differences in $N\text{-}N_2O$ and $\delta^{15}N\text{-}N_2O$ patterns can be attributed to N_2O reduction.

Summer period shows nearly the same distributions of $\delta^{15}N\text{-}N_2O$, $\delta^{15}N^{\alpha}\text{-}N_2O$, $\delta^{15}N^{\beta}\text{-}N_2O$ and $\delta^{18}O\text{-}N_2O$ (green circles, Fig. 5 C), except the slight decrease in $\delta^{18}O\text{-}N_2O$ at the interval which corresponds to sampling locations *5* and *4*.

In winter the patterns between $\delta^{15}N\text{-}N_2O$, $\delta^{15}N^{\alpha}\text{-}N_2O$, $\delta^{15}N^{\beta}\text{-}N_2O$ and $\delta^{18}O\text{-}N_2O$ (green circles, Fig. 5 C) are identical with the obvious increase at the deeper aquifer layers which corresponds to sampling point *1* (Pz13). This indicates that N_2O reduction dominates N_2O production in the deeper part of the aquifer. At the same time, N_2O production exceeds its consumption or occurs to the same extent at the upper part of the aquifer.

3.3. Potential rates of nitrification and denitrification processes obtained from laboratory incubation experiment

The results of the isotope analyses of $^{15}N\text{-}NO_3^-$, $^{15}N\text{-}N_2O$ and $^{15}N\text{-}N_2$ have not highlighted any considerable enrichment of respective compounds between different time spans. This indicates that nitrification or denitrification processes did not occur at significant rates in the bottles during the incubation experiments. The maximal analytical errors of the $^{15}N\text{-}NO_3^-$, $^{15}N\text{-}N_2O$, and $^{15}N\text{-}N_2$ analyses were ± 2‰, ± 0.14‰ and ± 0.1‰. The detection limits were: 1) for nitrification – 2.7 nmol/L/h and 2) for denitrification – 2.7 nmol/L/h for N_2 and 0.0002 nmol/L/h for N_2O.

4. Discussion

4.1. Evidence of N_2O production and consumption processes obtained from the analyses of ambient groundwater samples

According to the results, both N_2O production and consumptions processes occur in the chalk aquifer. The fact that N as an initial substrate originates from different sources at different depths complicates the distinction between nitrification and denitrification as well as between N_2O production and consumption mechanisms.

At SGB, the similarity between $\delta^{15}N\text{-}N_2O$ and $\delta^{15}N^{\beta}\text{-}N_2O$ in the summer campaign means that the isotopic signature of N_2O is not determined by N_2O reduction. In the winter campaign, simultaneous increase in N_2O isotopomers values (with more pronounced increase in $^{15}N^{\alpha}$) and $\delta^{18}O\text{-}N_2O$ at levels *7* and *6* indicates (Park et al., 2011) the occurrence of N_2O reduction processes at the bottom part of the aquifer. This is also supported by the drastic decrease in the concentration of NO_3^- at sampling point *6* in comparison to *7*. The opposite patterns of NO_3^- and N_2O concentrations in the deep part of the aquifer both in summer and winter periods provide additional evidence of reduction processes (Minamikawa et al., 2011).

At Bovenistier, it could be concluded that N_2O production processes dominate over its consumption based on the similarities in the distributions of N isotopes, isotopomers, and $N\text{-}N_2O$ concentrations along the vertical profile. Intensive N_2O consumption is revealed only in the deep part of the aquifer (Pz13) during the winter campaign. This observation is probably related to significant NO_3^- input which stimulated denitrification process and allowed to detect N_2O at measureable levels.

As a first conclusion, despite of the occurrence of aerobic conditions at SGB and Bovenistier, both production and consumption processes govern the dynamics of N_2O, with the reduction processes being more pronounced in the deeper part of the aquifer. Such conclusions are supported by the fact that there is more and more evidence of denitrifiers being capable of using both DO and NO_3^- as electron acceptors (Zhu et al., 2019). Moreover, there are studies which suggest the presence of micro anaerobic hotspots in total aerobic environments capable of supporting denitrification processes (Well et al., 2012).

4.2. Evidence of N_2O production and consumption processes from laboratory incubation experiments

The results show that our previous hypothesis about the simultaneous occurrence of both nitrification and denitrification processes in the aquifer might not explain the SP values of N_2O measured in groundwater samples collected during the regional and local investigations. Consequently, on the one hand the availability of N_2O in the aquifer might be explained by the infiltration of N_2O produced by nitrification and denitrification processes occurring within the other parts of the aquifer. Alternatively, there might exist a discrepancy between real aquifer conditions and laboratory experiments. In particular, in the aquifer, groundwater is in permanent contact with biofilms attached to the rocks materials, while groundwater samples collected in piezometers for incubation might not represent the real complexity of the subsurface environment. To investigate this, it would be needed to collect large volumes of groundwater to extract the available bacterial biomass and analyze it in order to determine the expression of nitrifying and denitrifying genes, which might help to obtain better insight into the qualitative diversity of biofilm biotope, since it is expected that there exists a constant flux of bacteria between biofilm and water layers.

5. Conclusions

This study applied stable isotope analyses and laboratory design tracer experiments in order to clarify the origin of N_2O in groundwater. The results of measurements of N isotope parameters in ambient groundwater samples and laboratory incubations are controversial.

It is difficult to differentiate between the roles of nitrification and denitrification in N_2O production because N isotopic signatures and SP values measured in collected groundwater are overlapping. At the same time, N_2O reduction, which is related solely to denitrification, could be identified based on positive values of $\delta^{15}N\text{-}N_2O$, high values of $\delta^{18}O\text{-}N_2O$ (> 35‰) and enrichment in $^{15}N^{\alpha}\text{-}N_2O$. In particular, at one of the examined locations (Pz 13) SP, $\delta^{15}N\text{-}N_2O$ and $\delta^{18}O\text{-}N_2O$ values of ambient groundwater showed ranges typical for complete denitrification (with N_2O reduction) which coincide with the lower DO levels measured at this location.

Since direct measurement of the magnitude of nitrification and denitrification processes within the aquifer is not possible at the majority of selected locations due to the high groundwater fluxes, it was decided to conduct laboratory bottle incubation experiments to determine the potential rates of respective processes. Those results did not detect nitrification and denitrification in the bottles and this might be related to the fact that N_2O availability in groundwater is determined by nitrification and denitrification processes in the unsaturated zone. However, the results draw our attention since at Pz 13 the SP and $\delta^{15}N\text{-}N_2O$ values were significantly different from values obtained at other locations as they showed ranges typical for N_2O reduction which coincide with low DO levels in groundwater at this location.

Those three facts suggest that the best explanation might be the discrepancy between real aquifer conditions and lab design studies. Laboratory studies were conducted under controlled conditions but the aquifer conditions are more complex. Not only the amount of bacteria in the collected samples could differ, but reaction rates during the experiments and in the aquifer actually differ. Therefore, the isotopic signatures of N_2O in the aquifer might indicate that denitrification occurs in the aquifer but the responsible bacteria were not present in sufficient quantity in the collected groundwater samples because they mostly reside in biofilms attached to the surface of the rocks materials.

To sum up, the solitary application of isotope and isotopomer analyses together with hydrochemical evidence can provide the information only about production or consumption of N_2O in the subsurface. Under the heterogeneous conditions prevailing in the subsurface, the SP values

and N isotope signatures are the result of mixing between continuous transformation and transport processes of N compounds driven from different sources. Consequently, it is difficult to draw definitive conclusions about the location and extent of key functional zones in N cycle dynamics based only on the isotope and isotopomer datasets.

Evidences from laboratory incubation experiments should be verified by additional *in situ* tracer experiments at locations that are characterized by low groundwater fluxes that allows leaving a tracer in subsurface for at least several hours. In addition, it will be useful to conduct microbiological studies of the biomass extracted from groundwater which will allow having better understanding about activity of subsurface biofilm biotope. Finally, it is important to emphasize that microbiological findings should not be focused on the evidence of abundance of certain organisms or enzymes, which might be misleading, but rather on determining their actual activity based on mRNAs or protein.

Declaration of Competing Interest

none.

Acknowledgments

This project has received funding from the European Union's Horizon 2020 research and innovation programme under the Marie Skłodowska-Curie grant agreement No 675120. Los Gatos Research OA-ICOS was funded by the Fonds National de la Rechecherche Scientifique (FNRS) (22547486). AVB is a Research Director at the FNRS.

References

Anderson, B., Bartlett, K.B., Frolking, S., Hayhoe, K., Jenkins, J.C., Salas, W.A., 2010. Methane and Nitrous Oxide Emissions from Natural Sources.

Borges, A.V., Darchambeau, F., Teodoru, C.R., Marwick, T.R., Tamooh, F., Geeraert, N., Okuku, E., 2015. Globally significant greenhouse-gas emissions from African inland waters. Nat. Geosci. 8 (8), 637.

Brouyère, S., Dassargues, A., Hallet, V., 2004. Migration of contaminants through the unsaturated zone overlying the Hesbaye chalky aquifer in Belgium: a field investigation. J. Contam. Hydrol. 72 (1–4), 135–164.

Clark, I., 2015. Contaminant geochemistry and isotopes. In: Groundwater Geochemistry and Isotopes. Taylor & Francis Group, LLC, Boca Raton, FL.

Davidson, E.A., 2009. The contribution of manure and fertilizer nitrogen to atmospheric nitrous oxide since 1860. Nat. Geosci. 2 (9), 659–662.

Fisher, T.R., Fox, R.J., Gustafson, A.B., Lewis, J., Millar, N., Winsten, J.R., 2018. Fluxes of nitrous oxide and nitrate from agricultural fields on the Delmarva Peninsula: N biogeochemistry and economics of field management. Agric. Ecosyst. Environ. 254, 162–178.

Fox, R.J., Fisher, T.R., Gustafson, A.B., Jordan, T.E., Kana, T.M., Lang, M.W., 2014. Searching for the missing nitrogen: biogenic nitrogen gases in groundwater and streams. J. Agric. Sci. 152 (S1), 96.

Gardner, J.R., Fisher, T.R., Jordan, T.E., Knee, K.L., 2016. Balancing watershed nitrogen budgets: accounting for biogenic gases in streams. Biogeochemistry 127 (2–3), 231–253.

Goderniaux, P., Brouyère, S., Wildemeersch, S., Therrien, R., Dassargues, A., 2015. Uncertainty of climate change impact on groundwater reserves–application to a chalk aquifer. J. Hydrol. 528, 108–121.

Guo, L., Wang, X., Diao, T., Ju, X., Niu, X., Zheng, L., Han, X., 2018. N2O emission contributions by different pathways and associated microbial community dynamics in a typical calcareous vegetable soil. Environ. Pollut. 242, 2005–2013.

Hama, T., Miyazaki, T., Ogawa, Y., Iwakuma, T., Takahashi, M., Otsuki, A., Ichimura, S., 1983. Measurement of photosynthetic production of a marine phytoplankton population using a stable 13 C isotope. Mar. Biol. 73 (1), 31–36.

Hasegawa, K., Hanaki, K., Matsuo, T., Hidaka, S., 2000. Nitrous oxide from the agricultural water system contaminated with high nitrogen. Chemosphere-Global Change Science 2 (3), 335–345.

Hinkle, S.R., Tesoriero, A.J., 2014. Nitrogen speciation and trends, and prediction of denitrification extent, in shallow US groundwater. J. Hydrol. 509, 343–353.

IPCC, 2016. In: Edenhofer, O., Pichs-Madruga, R., Sokona, Y., Farahani, E., Kadner, S., Seyboth, K., Minx, J.C. (Eds.), Climate Change 2014: Mitigation of Climate Change. Contribution of Working Group III to the Fifth Assessment Report of the Intergovernmental Panel on Climate Change.

Jahangir, M.M., Johnston, P., Barrett, M., Khalil, M.I., Groffman, P.M., Boeckx, P., Richards, K.G., 2013. Denitrification and indirect N2O emissions in groundwater: hydrologic and biogeochemical influences. J. Contam. Hydrol. 152, 70–81.

Jurado, A., Borges, A.V., Pujades, E., Hakoun, V., Otten, J., Knoeller, K., Brouyere, S., 2018. Occurrence of greenhouse gases in the aquifers of the Walloon Region (Belgium). Sci. Total Environ. 619, 1579–1588.

Koba, K., Osaka, K., Tobari, Y., Toyoda, S., Ohte, N., Katsuyama, M., Kim, S.J., 2009. Biogeochemistry of nitrous oxide in groundwater in a forested ecosystem elucidated by nitrous oxide isotopomer measurements. Geochim. Cosmochim. Acta 73 (11), 3115–3133.

McIlvin, M.R., Altabet, M.A., 2005. Chemical conversion of nitrate and nitrite to nitrous oxide for nitrogen and oxygen isotopic analysis in freshwater and seawater. Anal. Chem. 77 (17), 5589–5595.

Michener, R., Lajtha, K., 2007. Tracing anthropogenic inputs of nitrogen to ecosystems. In: Kendall, C., Elliott, E., M. & Wankel, S., D. (Eds.), Stable Isotopes in Ecology and Environmental Science, 2nd ed. Blackwell Publishing Ltd., Carlton, Victoria, pp. 375–449.

Minamikawa, K., Nishimura, S., Nakajima, Y., Osaka, K.I., Sawamoto, T., Yagi, K., 2011. Upward diffusion of nitrous oxide produced by denitrification near shallow groundwater table in the summer: a lysimeter experiment. Soil Science and Plant Nutrition 57 (5), 719–732.

Mosier, A.R., Schimel, D.S., 1993. Nitrification and denitrification. In: Nitrogen Isotope Techniques. Academic Press, pp. 181–208.

Nikolenko, O., Orban, P., Jurado, A., Morana, C., Jamin, P., Robert, T., Brouyère, S., 2019. Dynamics of greenhouse gases in groundwater: hydrogeological and hydrogeochemical controls. Appl. Geochem. 105, 31–44.

Orban, P., Brouyère, S., Batlle-Aguilar, J., Couturier, J., Goderniaux, P., Leroy, M., Malozewski, P., Dassargues, A., 2010. Regional transport modelling for nitrate trend assessment and forecasting in a chalk aquifer. J. Cont. Hydrol. 118, 79–93.

Ostrom, N.E., Pitt, A., Sutka, R., Ostrom, P.H., Grandy, A.S., Huizinga, K.M., Robertson, G.P., 2007. Isotopologue effects during N2O reduction in soils and in pure cultures of denitrifiers. Journal of Geophysical Research: Biogeosciences 112 (G2).

Park, S., Pérez, T., Boering, K.A., Trumbore, S.E., Gil, J., Marquina, S., Tyler, S.C., 2011. Can N2O stable isotopes and isotopomers be useful tools to characterize sources and microbial pathways of N2O production and consumption in tropical soils? Glob. Biogeochem. Cycles 25 (1).

Ryabenko, E., Altabet, M.A., Wallace, D.W., 2009. Effect of chloride on the chemical conversion of nitrate to nitrous oxide for δ15N analysis. Limnol. Oceanogr. Methods 7 (7), 545–552.

Tirez, K., Brusten, W., Widory, D., Petelet, E., Bregnot, A., Xue, D., Bronders, J., 2010. Boron isotope ratio (δ11B) measurements in Water Framework Directive monitoring programs: comparison between double focusing sector field ICP and thermal ionization mass spectrometry. J. Anal. At. Spectrom. 25 (7), 964–974.

Wassenaar, L.I., Douence, C., Altabet, M.A., Aggarwal, P.K., 2018. N and O isotope (δ15Nα, δ15Nβ, δ18O, δ17O) analyses of dissolved NO3− and NO2− by the cd-azide reduction method and N2O laser spectrometry. Rapid Commun. Mass Spectrom. 32 (3), 184–194.

Well, R., Eschenbach, W., Flessa, H., von der Heide, C., Weymann, D., 2012. Are dual isotope and isotopomer ratios of N2O useful indicators for N2O turnover during denitrification in nitrate-contaminated aquifers? Geochim. Cosmochim. Acta 90, 265–282.

Widory, D., Kloppmann, W., Chery, L., Bonnin, J., Rochdi, H., Guinamant, J.L., 2004. Nitrate in groundwater: an isotopic multi-tracer approach. J. Contam. Hydrol. 72 (1–4), 165–188.

World Meteorological Organization, 2018. MO Greenhouse Gas Bulletin (GHG Bulletin): The state of greenhouse gases in the atmosphere based on global observations through 2017.

Xue, D., Botte, J., De Baets, B., Accoe, F., Nestler, A., Taylor, P., Boeckx, P., 2009. Present limitations and future prospects of stable isotope methods for nitrate source identification in surface-and groundwater. Water Res. 43 (5), 1159–1170.

Zhou, W., Lin, J., Tang, Q., Wei, Z., Schwenke, G., Li Liu, D., Yan, X., 2019. Indirect N2O emissions from groundwater under high nitrogen-load farmland in eastern China. Environ. Pollut. 248, 238–246.

Zhu, X., Zhao, D., Pan, Z., Zhang, W., Ruan, X., 2019, July. Characteristics of an aerobic denitrifier isolated from unconfined aquifer. In: IOP Conference Series: Earth and Environmental Science, Vol. 300. IOP Publishing, p. 052009. No. 5.